# Influence of Al substitution on the atomic and electronic structure of Si clusters by density functional theory and molecular dynamics simulations

Chiranjib Majumder* and S. K. Kulshreshtha
*Novel Materials and Structural Chemistry Division, Bhabha Atomic Research Center, Trombay, Mumbai 400 085, India*
(Received 9 September 2003; revised manuscript received 18 November 2003; published 30 March 2004)

A systematic theoretical study of the equilibrium geometry and energetics of $Si_n$ and $Si_{n-1}Al$ clusters has been carried out using a combination of the density functional theory and molecular dynamics simulation under the local spin density (LSD) approximation. The lowest energy isomer thus obtained is further used to evaluate the total energy using *ab initio* quantum chemical technique at the second-order Møller-Plesset [MP2/6-31G(d)] level taking all electrons into account. Based on the comparative study between $Si_n$ and $Si_{n-1}Al$ clusters it is found that the ground-state geometries of the $Si_{n-1}Al$ clusters are almost similar to that of $Si_n$ clusters with the Al atom replacing one of the Si atoms with small local distortion. However, significant differences have been observed in their electronic structure and the fragmentation behavior. The average binding energies of the $Si_n$ and $Si_{n-1}Al$ clusters vary in a similar way with slightly higher values for the $Si_n$ clusters. Clusters of both these series with $n=4,6,10$ show higher stability as compared to its neighboring clusters. The dissociation energies calculated for Al and Si atoms suggest that the evaporation of an Al atom is easier than that of Si. However, a comparison of the dissociation energies of Si atoms from $Si_n$ and $Si_{n-1}Al$ clusters revealed that for $n=4,6,10$, the evaporation of Si atoms from the $Si_{n-1}Al$ cluster requires more energy than that of the corresponding $Si_n$ cluster implying an improvement in the bond strength between Si-Si bonds for these $Si_{n-1}Al$ clusters due to Al substitution in $Si_n$. Finally, a good agreement of our results and the previously published results on Si clusters gives us the confidence to believe the good prediction of our results on the $Si_{n-1}Al$ clusters.

DOI: 10.1103/PhysRevB.69.115432 PACS number(s): 73.22.−f, 36.40.Cg, 36.40.Qv, 36.40.Ei

## INTRODUCTION

The study of atomic clusters has become an active area of research during the last two decades. Among different clusters, Si clusters have been studied most extensively using both theoretical and experimental techniques.[1–26] This is due to its technological relevance towards the development of nanoelectronics, which gives an extra impetus to understand the properties of silicon with its miniaturization.[1–3] Photodissociation[4–6] and collision-induced dissociation[7–9] experiments have shown that both $Si_6$ and $Si_{10}$ have exceptional stability, consistent with their ''magic'' behavior observed in the mass spectra of Si clusters.[10] Several spectroscopic studies viz., photoelectron spectroscopy, Raman and infrared spectroscopy, etc., have been carried out to understand the atomic structure of small silicon clusters.[11–14] However, the analysis of spectroscopic data becomes extremely complex as the size increases beyond four atoms. The computational studies provide an alternative to understand the geometries of relatively large clusters. *Ab initio* molecular orbital theory is commonly used to obtain direct information about the ground-state geometries of atomic and molecular clusters. Raghavachari and co-workers have systematically studied small silicon clusters using molecular-orbital theory taking all electrons into account.[15–20] In these calculations they have optimized several isomers at the HF/6-31G(d) level, followed by a total energy calculation at Møller-Plesset (MP) levels MP2, MP3, and MP4 with the polarized 6-31G(d) basis set.

Other than *ab initio* all electron methods, plane wave based pseudopotential approach under the density functional theory formalism has also been employed by several workers to obtain the ground-state geometries and properties of silicon clusters. Due to the advantage of using pseudopotentials (neglecting the core electrons) this method can be used for the calculation of larger clusters. However, it needs to be mentioned that the determination of global minimum is a challenging problem as the number of local minima increases significantly with increase in cluster size. The simulated annealing technique has been used to alleviate this problem.[21–26]

Although extensive investigations have been carried out on the geometry and energetics of the homoatomic silicon clusters, similar studies for the heteroatomic systems are very few. The problem of the metal-silicon bond has been the topic of a number of experimental[27–29] and theoretical[30–33] studies for bulk metal-silicon systems. In the pioneering work of Beck,[34] the metal-silicon clusters $MSi_n$ ($M=$Cu, Cr, Mo, and W) were generated using laser vaporization technique. The mass spectrum of $CuSi_n$ ($6<n<12$) showed exceptional stability for $CuSi_{10}$ clusters. More recently, Scherer and co-workers[35–37] produced noble-metal-doped silicon clusters $M@Si_n$ for $M=$Cu, Ag, and Au. In another study, Hiura *et al.*[38] have reported experimental evidence of the formation of stable metal-encapsulating silicon cage cluster ions for $MSi_n$ (with $M=$Hf, Ta, W, Re, Ir, etc., and $n=14$, 13, 12, 11, 9, respectively) and proposed a structural model of regular hexagonal prism for $WSi_{12}$ with the W atom at the center. This finding aroused significant interest to search for cagelike Si clusters stabilized by metal atom incorporation. Stimulated by the experimental findings, several computational investigations have been performed for metal-doped

 ©2004 The American Physical Society

silicon clusters.[39–47] Very recently, Kumar and Kawazoe[48,49] reported several types of metal-encapsulating caged structures with high stability for a series of $M@Si_n$ clusters ($n=14–17$, $M=$Cr, Mo, W, Fe, Ru, Os, Ti, Zr, Hf). Following this work, a number of cagelike structures for the Si cluster have been reported by other workers.[50] From the above studies it is clear that the nature of metal atoms and its interaction with Si plays an important role to modify the bonding and thereby structure of host cluster.

Although several reports are available on the interaction of a transition metal (TM) atom with Si clusters similar investigations with simple metal atoms are very few. Kishi *et al.*[51] carried out a combined experimental and theoretical study of $NaSi_n$ ($n<7$), and found that the Na atom acts as an electron donor to the $Si_n$ framework and the most stable isomer of $NaSi_n$ retains the framework of corresponding $Si_n$ cluster nearly unchanged upon the adsorption of Na.

A recent study has revealed that the interaction of an Al atom with Si nanowire significantly enhanced its electrical conductivity.[52] Reports are also available where Al atoms form an ordered array of magic clusters[53] on the surfaces of Si(111) and the formation of Al-Si nanowires.[54] Motivated by these results, we thought it will be interesting to understand the nature of chemical bonding between Si and Al atoms in these systems at the atomic scale. The objective of this study is to understand the electronic interaction of Al atoms on the Si clusters and to compare the geometric and electronic structure between $Si_n$ and $Si_{n-1}Al$ clusters. In the first part of this study we have calculated the geometries and energetics of $Si_n$ ($n=2–11$) clusters. In order to check the reliability of our calculation method, these results were compared with the available experimental values. This was followed by the geometry and electronic structure optimizations for $Si_{n-1}Al$ clusters. In order to understand the nature of interaction between an Al atom and Si clusters we have adopted three different sites of adsorption of the Al atom on the Si clusters as discussed below.

## COMPUTATIONAL APPROACH

The interaction of an impurity atom with a homoatomic cluster can lead to three different possibilities viz., (a) the impurity atom can occupy the center of the cage formed by the host cluster (*endohedral*), (b) the impurity atom can adsorb on the surface of the host cluster (*exohedral*), and (c) the impurity atom can replace one atom from the network of the host cluster (*substitutional*).

For $Si_n$ clusters, we have examined a number of possible isomeric structures as predicted earlier by several groups based on Hartree-Fock and density functional theory.[15–26] For $Si_{n-1}Al$ clusters, similar starting geometries with one Si atom replaced by an Al atom at different positions were considered along with the endohedral and exohedral configurations as mentioned in (a) and (b). Initially the geometries were optimized using density functional theory formalism under the local spin density (LSD) approximation.[55] We have used the norm-conserving pseudopotentials of Bachelet *et al.*[56] with the Kleimann and Bylander decomposition[57] to describe the electron-ion interaction and a plane wave basis set to represent the wave function. The cutoff energy for the plane wave expansion was set up to 25 Ry for the calculation of the total energy. The exchange correlation energy used here has been taken from the parametrized form of Ceperley and Alder.[58] The geometries thus constructed were optimized until the forces are minimized to $10^{-4}$ (Hartrees/Bohr). In order to confirm the lowest energy isomer we have also applied the simulated annealing technique, i.e., heating the initial configurations up to 1000 K, allowing to relax the structure at this temperature for $\sim$5 ps and then slowly cooling it to 0 K. The geometries thus obtained were compared with those obtained by directly minimizing several low-energy isomers and the structure with lowest energy was considered as the ground-state geometry.

Finally, total energy calculations were carried out for the lowest-energy isomers at the level of the Møller-Plesset perturbation theory incorporating the energy correlation effects truncated at second order (MP2).[59–61] A standard split-valence basis set with polarization functions [6-31G(d)] was employed for this purpose. These calculations were carried out using GAMESS software.[62]

## RESULTS AND DISCUSSION

**$Si_n$ clusters**. All neutral Si clusters calculated in this study have singlet spin multiplicity in the ground state except $Si_2$, which favors triplet spin state over singlet by 0.80 eV of total energy. The lowest-energy structures of $Si_n$ clusters correspond to an isosceles triangle, a planar rhombus, capped bent rhombus, an edge capped trigonal-bipyramid (TBP), a pentagonal-bypyramid (PBP) for $Si_3$, $Si_4$, $Si_5$, $Si_6$, and $Si_7$, respectively. For $Si_8$ cluster, bicapped trigonal-antiprism is lower in energy than capped PBP structure by 0.68 eV of energy. The lowest-energy structure of the $Si_9$ cluster consists of two distorted rhombus stacked with an additional atom capping from the top. For $Si_{10}$ and $Si_{11}$ clusters, the tetracapped-trigonal-prism (TTP) and pentacap-trigonal-prism (PTP) have been found to be the lowest-energy structures.

In Table I we have summarized the binding energies per atom of $Si_n$ clusters obtained in the present calculations using a combination of DFT-LDA and MP2/6-31G(d) methods along with the available experimental values.[63] The total energies obtained in this way may not correspond to the real MP2 minima as the geometries were taken from the LDA calculations. To check the accuracy of this scheme we have compared our results with the recently published results of Zhu and Zenga,[64] where they have optimized the geometries of small Si clusters at the MP2/6-31G(d) level. An excellent agreement between these results and our calculated values indicates that the geometries obtained using the DFT-LDA method can give a good estimate for the ground-state structures. This has motivated us to proceed further to calculate the geometries and energetics of Al substituted Si clusters using the same method. The trend in the binding energy under both these techniques is similar, i.e., initially it increases up to $n=7$ and then there is a small dip at $n=8$, which is followed by an increase up to $n=10$ and a fall at $n=11$. From the comparison of these results with the experimental

TABLE I. Comparison of the binding energies of small Si clusters obtained using DFT calculations under local density approximation (LDA) and the second-order Moller-Plesset [MP2/6-31G(d)] level taking all electrons into account. Experimental values listed in the last column are taken from Ref. 63.

| $n$ | $Si_n$ (LDA) | $Si_n$ (MP2) | $Si_n$ (MP2)[a] | Exp. |
|---|---|---|---|---|
| 2 | 1.89 | 1.31 | 1.29 | 1.61 |
| 3 | 2.79 | 2.17 | 2.15 | 2.45 |
| 4 | 3.34 | 2.77 | 2.74 | 3.10 |
| 5 | 3.60 | 2.96 | | 3.42 |
| 6 | 3.78 | 3.23 | 3.18 | 3.60 |
| 7 | 3.92 | 3.36 | 3.31 | |
| 8 | 3.85 | 3.25 | 3.20 | |
| 9 | 3.97 | 3.38 | 3.33 | |
| 10 | 4.07 | 3.54 | 3.50 | |
| 11 | 3.98 | 3.43 | 3.40 | |

[a]The binding energies obtained by optimizing the geometries using MP2/6-31G(d) level of theory (Ref. 64).

values it can be inferred that while LDA overestimates the binding energy values, MP2 calculations underestimate it.

**$Si_{n-1}Al$ clusters**. All the $Si_{n-1}Al$ clusters showed ground-state spin multiplicity to a doublet except for the Si-Al dimer, for which the quintet state is 1.25 eV lower in energy than the doublet. In Fig. 1 we have shown a few low-lying isomers of the $Si_{n-1}Al$ clusters, which are within energy difference of $\sim$1.5 eV for $3 \leqslant n \leqslant 11$. Salient features of these geometries are discussed below.

The geometries of Si-Al, $Si_2Al$, and $Si_3Al$ clusters are planar having shapes of linear, isosceles triangle, and rhombus, with the corresponding interatomic separations between Al and Si atoms of 2.437, 2.50, and 2.49 Å, respectively. The smallest interatomic separation between Si atoms is 2.20 Å for $AlSi_2$ and for $AlSi_3$ it is 2.29 Å.

For the $Si_4Al$ cluster, we have investigated several isomeric structures obtained for $Si_5$ and those reported for the Cu-doped $Si_4$ cluster recently.[65] Capped bent rhombus (113°) formed by four Si atoms and the Al atom connected to the long diagonal Si atoms shows the lowest-energy configuration. The smallest Si-Al and Si-Si distance are found to be 2.59 and 2.33 Å, respectively. Other higher-energy isomers consist of flattened trigonal bipyramid, trigonal face capped rhombus, and square pyramid structure, as shown in Fig. 1.

Several initial geometries were considered to obtain the lowest-energy structure of the $Si_5Al$ cluster. For the $Si_6$ neutral cluster, the edge capped trigonal bipyramid ($C_{2v}$) and crossed rhombus ($D_{4h}$) lie very close to each other as regards their total energy. The comparison of total energy among various possible isomeric structure suggests that the $Si_5$ cluster forms a trigonal bipyramid and the Al atom occupies the base plane by sharing one arm of the base triangle. The distance between Al and two Si atoms is 2.46 Å. The bond lengths between Si atoms from the apex to the base plane and among the base plane atoms are 2.47 and 2.42 *A* Å, respectively. In order to understand the growth motif we can view this structure as bicapped bent rhombus where Si and Al atoms are capping the $Si_4$ rhombus from opposite site. It is noted that due to the asymmetric capping the rhombus is bent by 153°, which is larger than that for the $Si_4Al$ cluster where Al atom was capping from one side.

For the $Si_6Al$ cluster, several isomers with pentagonal bipyramid structure and capped octahedron were considered. The lowest-energy isomer shows pentagonal bipyramid structure with the Al atom occupying one corner of the base pentagon. The bond lengths between Al and Si atoms in the base plane and the vertex to the base are 2.55 and 2.59 Å, respectively. It is clear from this figure that for the $Si_6Al$ cluster, edge capped octahedron isomers are higher in energy than PBP isomers. We have also considered the initial geometry with Al encapsulated in the $Si_6$ octahedron. After the geometry optimization the final structure suggests that Al atom cannot be trapped inside or in other words there is no metastable state where Al atom can be encapsulated inside the $Si_6$ octahedron. For the $Si_7Al$ cluster the lowest-energy structure was found to be a capped pentagonal bipyramid where the Al atom is capping one of the triangular faces of the PBP. This structure is different from the $Si_8$ cluster, which favors bicapped trigonal antiprism as the lowest-energy structure. The distance between Al and Si atoms was found to be 2.71 Å. In order to further ensure we have compared the total energies of the $Si_8$ and $Si_7Al$ cluster with both geometries of capped pentagonal bipyramid and bicapped trigonal antiprism at the MP2 level of theory. These results showed that while the capped PBP is 0.38 eV lower in energy for the $Si_7Al$ cluster, bicapped trigonal antiprism is 0.68 eV lower for the $Si_8$ cluster. Two other structures where the Al atom is occupying either one corner of the base pentagon or the vertex position of the PBP were found to be very close in energy with a difference of 0.06 eV.

For the $Si_8Al$ cluster several starting geometries similar to the isomers of the $CuSi_8$ cluster (Ref. 65) and isomers of $Si_9$ (Ref. 64) were optimized. No metastable state was obtained for an encapsulated $Si_8Al$ cluster where the Al atom could be trapped inside the cage of the $Si_8$ cluster. The lowest-energy structure appears to be a bicapped pentagonal bipyramid as obtained by changing the position of the Al atom at different Si sites. This structure is slightly different from the ground-state geometry of the $Si_9$ cluster (two rhombus stacked with an additional Si atom at the top). Another close lying isomer is a tricapped trigonal prism (TTP) is found to be 0.28 eV higher in energy than the bicapped pentagonal bipyramid structure.

The $Si_9Al$ cluster shows tetracapped trigonal prism as the lowest energy structure. This is also the ground-state geometry of the $Si_{10}$ cluster. The Al atom substitutes one Si atom from the triangular plane forming the prism. The other isomer where the Al atom is capping the triangular plane is 0.09 eV higher in energy. No structure, where the Al atom could be placed inside the TTP cage of the $Si_9$ cluster, was found to be stable. Two other isomers, which are spherical in shape, were found to be higher in energy than the lowest energy structure by 0.21 and 0.25 eV.

The $Si_{10}$ cluster has been predicted to be magic cluster due to its higher stability as compared to its adjacent clusters.

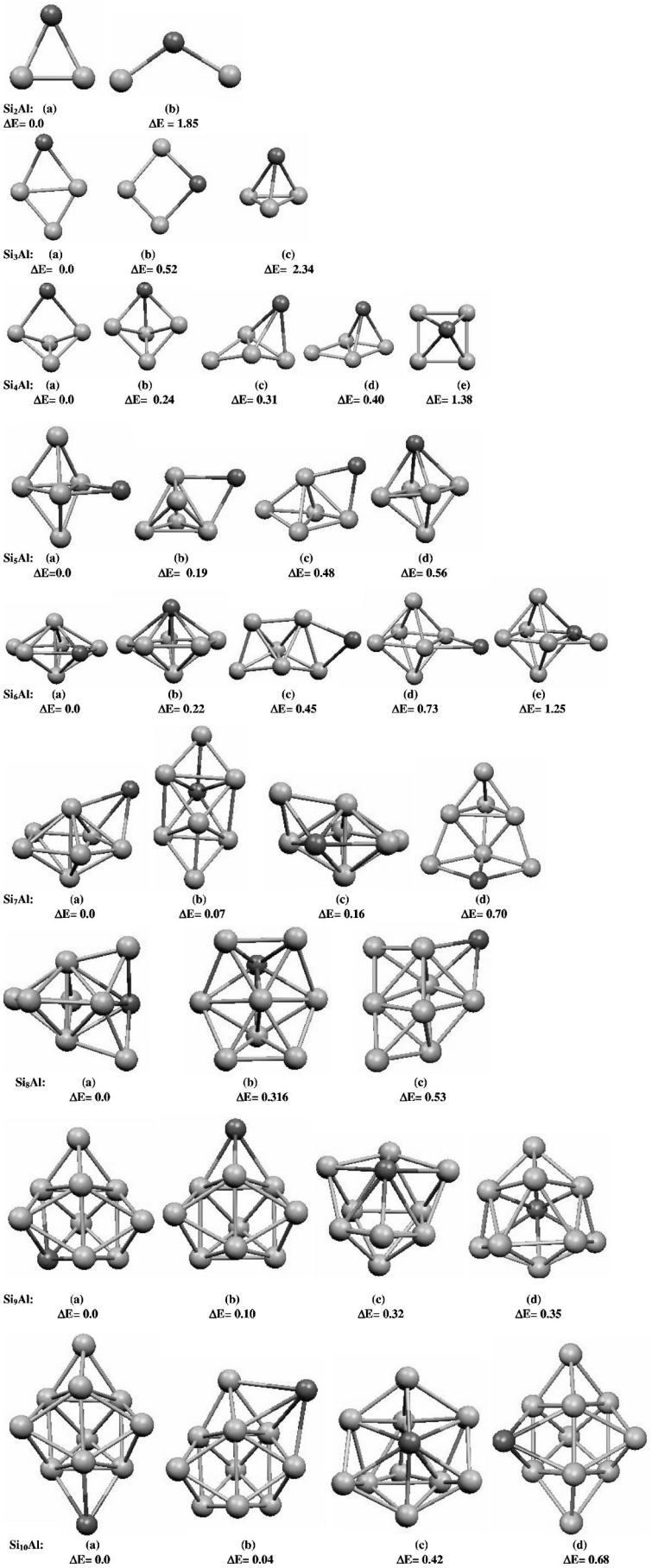


FIG. 1. Geometries of the low-lying isomers of the $Si_{n-1}Al$ cluster. Dark circle represents the Al atom. The isomers are organized in the order of their relative stability starting with the lowest energy isomer at the left. The relative stability of different isomers is expressed in terms of their energy difference (eV) with respect to the lowest-energy structure.

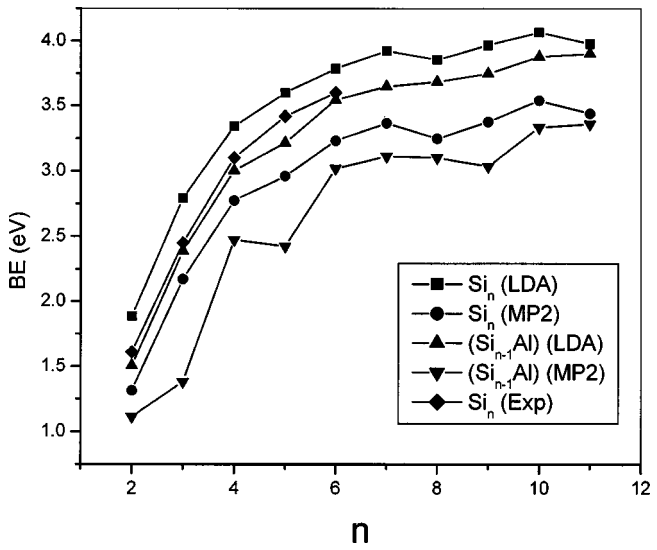


FIG. 2. Comparison of the binding energies of $Si_n$ and $Si_{n-1}Al$ clusters calculated using DFT and *ab initio* molecular orbital theory. Experimental values for $Si_n$ clusters are taken from Ref. 64.

The adsorption of the Al atom on the $Si_{10}$ cluster was carried out by capping the different faces of the $Si_{10}$ cluster (TTP) and also by replacing one atom from the $Si_{11}$ cluster at different substitutional sites. After comparing the energies of all these isomers the pentacap triangular prism structure was found to show the lowest energy structure for $Si_{10}Al$ cluster with where the Al atom is capping one of the triangular faces of the $Si_{10}$ cluster.

## ENERGETICS

**Binding energy:** In order to understand the relative stability of $Si_n$ and $Si_{n-1}Al$ clusters the binding energy per atom has been plotted in Fig. 2 as a function of total number of atoms present in the cluster. These binding energies are calculated as follows:

$$\mathrm{BE}(\mathrm{Si}_n) = 1/n[E(\mathrm{Si}_n) - n \times E(\mathrm{Si})]$$

$$\mathrm{BE}(\mathrm{Si}_{n-1}\mathrm{Al}) = 1/n[E(\mathrm{Si}_{n-1}\mathrm{Al}) - (n-1) \times E(\mathrm{Si}) - E(\mathrm{Al})].$$

It is clear from this figure that the binding energy increases as the size of the cluster grows with some exceptions of shallow minima corresponding to those clusters, which are relatively less stable as compared to their adjacent clusters. For example, the binding energy curve of the neutral $Si_n$ cluster suggests that the $Si_8$ cluster is less stable as compared to $Si_7$ or $Si_9$ cluster. Similarly, for $Si_{n-1}Al$ clusters, $Si_4Al$ and $Si_8Al$ are less stable as compared to their adjacent clusters.

**Fragmentation behavior:** The fragmentation behavior of a series of clusters bears significance in terms of understanding the abundance spectrum and the relative stability among smaller size clusters. We have calculated the fragmentation energy of $Si_n$ and $Si_{n-1}Al$ clusters as $E_F(\mathrm{Si}_n) = E(\mathrm{Si}_n) - E(\mathrm{Si}_{n-p}) - E(\mathrm{Si}_p)$ and $E_F(\mathrm{AlSi}_{n-1}) = E(\mathrm{AlSi}_{n-1}) - E(\mathrm{AlSi}_{n-1-p}) - E(\mathrm{Si}_p)$, respectively. In this calculation we have assumed that the fragmentation occurs along the lowest-energy pathways with no activation barrier.

In Table II we have listed all possible fragmentation pathways for $Si_n$ and $Si_{n-1}Al$ clusters (*except those related with the dissociation of an* Al *atom*) along with their fragmentation energies. Bloomfield *et al.* have carried out an experimental study to find out the fragmentation behavior of small Si clusters.[67] A good agreement between our calculated results with that of the experimental finding was obtained. Up to $n=8$, the most favored fragmentation channel for $Si_n$ cluster is to dissociate into $Si_{n-1}$ and Si atoms. Larger clusters favor to dissociate into two stable products. In one of our earlier studies, similar fragmentation pattern was also observed for tin clusters.[68] Most interestingly it has been noticed that in the presence of an Al atom in the matrix of small Si clusters, the fragmentation behavior changes significantly. From Table II it is clear that for $Si_{n-1}Al$ clusters, even for very small sizes, such as $n=4$ and 6, the evaporation of a Si atom is not the second lowest-energy channel (Al *atom removal is always the lowest-energy channel for* $Si_{n-1}Al$ *clusters*). This behavior is distinctly different from the corresponding $Si_n$ clusters. Figure 3 shows the plot for the dissociation energies of an Al or Si atom from the $Si_{n-1}Al$ clusters and these values have been compared with the energy required to remove a Si atom from $Si_n$ clusters. It has been found that the energy required to dissociate Si atom is higher than Al atom for $Si_{n-1}Al$ clusters. The clusters with $n=4$, 6, and 10 shows higher stability as compared to others for both the series. For $Si_n$ clusters with $n \leqslant 8$, Si atom evaporation has been found to be the lowest-energy channel. Larger clusters with $n>8$ favor to dissociate into two stable products. The energy required to dissociate a Si atom from $Si_{n-1}Al$ is higher than $Si_n$ for clusters with $n=4$, 6, 8, 10, and 11. This result indicates that for these clusters the bond strength between Si-Si bonds is more than others in this series.

**Ionization potential:** The ionization potential (IP) is an important parameter to understand the stability towards ejecting out one electron from its HOMO energy level to the continuum. According to Koopmans' theorem,[66] $E_{\mathrm{HOMO}} = -\mathrm{IP}$. The present calculations [MP2/6-31G(d)] predict that the IP of Si and Al atoms is 8.14 and 5.83 eV, respectively which is in good agreement with the experimental values reported (Si=8.15 and Al=5.98 eV).[69] After realizing such excellent agreement for the atomic ionization potential values of these two elements we have listed the HOMO energies of all $Si_n$ and $Si_{n-1}Al$ clusters presented in Table III. In order to verify the validity of the Koopman theorem the vertical ionization potentials (VIP) of these clusters were also calculated from the total energies calculated using the MP2 theory. The VIP corresponds to the difference in energy between neutral and cation clusters keeping the atomic positions unaltered. It is found that except for $n=2$ and 3, our calculated VIP's are in good agreement with the reported experimental values. In this context it is worth to mention that the experiment is done at finite temperature and the IP's measured in the experiments represent for certain ensemble

TABLE II. Fragmentation channels of the $Si_n$ and $AlSi_{n-1}$ clusters calculated under MP2/6-31G(d) level of theory. The second and third columns indicate the fragmentation products derived from the parent $Si_n$ cluster and the fifth and sixth columns indicate the fragmentation products derived from the parent $AlSi_{n-1}$ clusters. $E_F = E(Si_n) = E(Si_{n-p}) - E(Si_p)$; $E_F = E(AlSi_{n-1}) - E(AlSi_{n-1-p}) - E(Si_p)$.

| $n$ | $Si_{n-p}$ | $Si_p$ | $E_F$ (eV) | $AlSi_{n-p}$ | $Si_p$ | $E_F$ (eV) |
|---|---|---|---|---|---|---|
| 3 | $Si_2$ | Si | 3.931 | AlSi | Si | 1.963 |
| 4 | $Si_3$ | Si | 4.617 | $AlSi_2$ | Si | 5.792 |
| | $Si_2$ | $Si_2$ | 5.880 | AlSi | $Si_2$ | 5.088 |
| 5 | $Si_4$ | Si | 3.774 | $AlSi_3$ | Si | 2.285 |
| | $Si_3$ | $Si_2$ | 5.723 | $AlSi_2$ | $Si_2$ | 5.410 |
| | | | | AlSi | $Si_3$ | 3.443 |
| 6 | $Si_5$ | Si | 4.646 | $AlSi_4$ | Si | 6.055 |
| | $Si_4$ | $Si_2$ | 5.753 | $AlSi_3$ | $Si_2$ | 5.673 |
| | $Si_3$ | $Si_3$ | 6.439 | $AlSi_2$ | $Si_3$ | 7.534 |
| | | | | AlSi | $Si_4$ | 4.881 |
| 7 | $Si_6$ | Si | 4.232 | $AlSi_5$ | Si | 3.735 |
| | $Si_5$ | $Si_2$ | 6.212 | $AlSi_4$ | $Si_2$ | 7.123 |
| | $Si_4$ | $Si_3$ | 6.055 | $AlSi_3$ | $Si_3$ | 5.477 |
| | | | | $AlSi_2$ | $Si_4$ | 6.652 |
| | | | | AlSi | $Si_5$ | 4.842 |
| 8 | $Si_7$ | Si | 2.468 | $AlSi_6$ | Si | 3.071 |
| | $Si_6$ | $Si_2$ | 4.034 | $AlSi_5$ | $Si_2$ | 4.140 |
| | $Si_5$ | $Si_3$ | 4.750 | $AlSi_4$ | $Si_3$ | 6.264 |
| | $Si_4$ | $Si_4$ | 3.906 | $AlSi_3$ | $Si_4$ | 3.932 |
| | | | | $AlSi_2$ | $Si_5$ | 5.950 |
| | | | | AlSi | $Si_6$ | 3.267 |
| 9 | $Si_8$ | Si | 4.467 | $AlSi_7$ | Si | 2.561 |
| | $Si_7$ | $Si_2$ | 4.268 | $AlSi_6$ | $Si_2$ | 2.965 |
| | $Si_6$ | $Si_3$ | 4.570 | $AlSi_5$ | $Si_3$ | 2.770 |
| | $Si_5$ | $Si_4$ | 4.600 | $AlSi_4$ | $Si_4$ | 4.208 |
| | | | | $AlSi_3$ | $Si_5$ | 2.719 |
| | | | | $AlSi_2$ | $Si_6$ | 3.865 |
| | | | | AlSi | $Si_7$ | 1.596 |
| 10 | $Si_9$ | Si | 5.105 | $AlSi_8$ | Si | 6.109 |
| | $Si_8$ | $Si_2$ | 6.905 | $AlSi_7$ | $Si_2$ | 6.003 |
| | $Si_7$ | $Si_3$ | 5.443 | $AlSi_6$ | $Si_3$ | 5.144 |
| | $Si_6$ | $Si_4$ | 5.059 | $AlSi_5$ | $Si_4$ | 4.262 |
| | $Si_5$ | $Si_5$ | 5.931 | $AlSi_4$ | $Si_5$ | 6.544 |
| | | | | $AlSi_3$ | $Si_6$ | 4.182 |
| | | | | $AlSi_2$ | $Si_7$ | 5.742 |
| | | | | AlSi | $Si_8$ | 5.237 |
| 11 | $Si_{10}$ | Si | 2.453 | $AlSi_9$ | Si | 3.671 |
| | $Si_9$ | $Si_2$ | 4.891 | $AlSi_8$ | $Si_2$ | 7.114 |
| | $Si_8$ | $Si_3$ | 5.427 | $AlSi_7$ | $Si_3$ | 5.744 |
| | $Si_7$ | $Si_4$ | 3.279 | $AlSi_6$ | $Si_4$ | 4.199 |
| | $Si_6$ | $Si_5$ | 3.738 | $AlSi_5$ | $Si_5$ | 4.160 |
| | | | | $AlSi_4$ | $Si_6$ | 5.569 |
| | | | | $AlSi_3$ | $Si_7$ | 3.621 |
| | | | | $AlSi_2$ | $Si_8$ | 6.945 |
| | | | | AlSi | $Si_9$ | 4.441 |

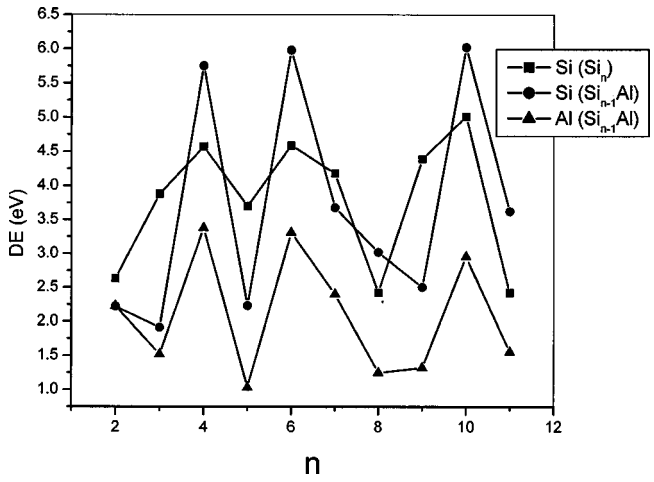


FIG. 3. The dissociation energies of Al and Si atoms from $Si_n$ and $Si_{n-1}Al$ clusters. The squares and circles represent dissociation energies of a Si atom from the $Si_n$ and $Si_{n-1}Al$ cluster, respectively. The triangles represent the dissociation energy of an Al atom from the $AlSi_{n-1}$ clusters.

of clusters and therefore isomer effects could be responsible for the differences in the theoretical and experimental values observed.

Comparison of the IP's between $Si_n$ and $Si_{n-1}Al$ clusters shows that the ionization potentials of $Si_n$ clusters decreases in presence of an Al atom. The reduction in the IP of $Si_{n-1}Al$ clusters can be attributed to the decrease in their HOMO energies as listed in Table III. The difference for $n=2$ is due to their difference in the spin multiplicity value which is triplet and quintet for $Si_2$ and AlSi, respectively. We have plotted the HOMO energy levels of $Si_n$ and $Si_{n-1}Al$ clusters as shown in Fig. 4. It is clear from this table that the HOMO energy levels of $Si_n$ clusters are lifted upwards (less negative) in the presence of the Al atom. This phenomenon is reflected in the reduction in the ionization potentials of Si clusters. In this context it is interesting to mention that in a recent work by Landmann *et al.*[52] it has been observed that

TABLE III. Comparison of the ionization potential values of $Si_n$ and $AlSi_{n-1}$ clusters obtained from the HOMO energy levels as well as the energy difference between the neutral and singly positive charge ions having fixed ionic positions.

| $n$ | ($Si_n$) HOMO | ($Si_n$) VIP | IP($Si_n$)[a] Exp. | ($Si_{n-1}Al$) HOMO | ($Si_{n-1}Al$) VIP |
|---|---|---|---|---|---|
| 2 | 7.61 | 7.41 | >8.49 | 7.91 | 7.59 |
| 3 | 7.97 | 8.02 | >8.49 | 6.76 | 6.13 |
| 4 | 8.25 | 8.33 | 7.97–8.49 | 7.90 | 7.04 |
| 5 | 8.01 | 8.21 | 7.97–8.49 | 7.03 | 6.30 |
| 6 | 8.29 | 7.88 | 7.97–8.49 | 7.88 | 7.30 |
| 7 | 8.12 | 8.09 | ~7.90 | 7.65 | 7.31 |
| 8 | 7.33 | 7.36 | 7.46–7.87 | 6.98 | 6.10 |
| 9 | 7.67 | 7.68 | 7.46–7.87 | 6.86 | 5.89 |
| 10 | 8.15 | 8.05 | ~7.90 | 8.02 | 7.21 |
| 11 | 6.83 | 7.20 | 7.46–7.87 | 6.57 | 5.49 |

[a]Experimental values from Ref. 70.

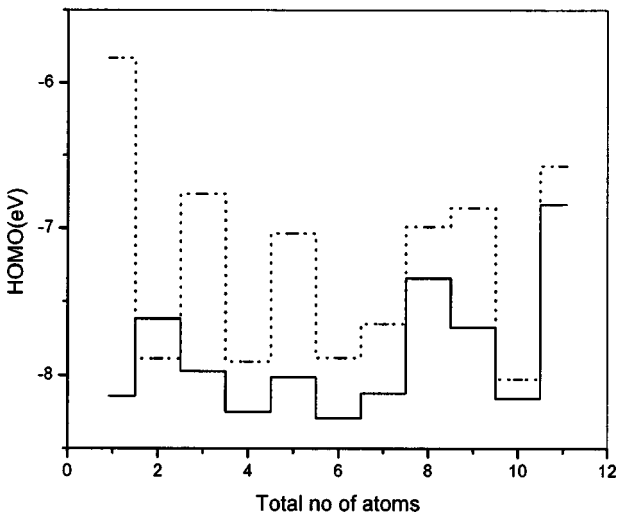


FIG. 4. The HOMO energy levels of the $Si_n$ (solid lines) and $Si_{n-1}Al$ (dotted lines) clusters calculated using MP2/6-31G(d) level of theory.

doping of an Al atom in the Si nanowire, assembled from the $Si_{24}$ or $Si_{96}$ clusters, enhances the electronic conductivity significantly. This has been explained due to the increase in the density of states by the incorporation of the Al atom. In the present study, the upward shift in the HOMO energy levels of the Al atom incorporated Si clusters bear an implication to corroborate the above phenomenon.

## CONCLUSION

In this work we have carried out the geometry optimization for $Si_n$ and $Si_{n-1}Al$ clusters using density functional theory under the local spin density approximation to account for the exchange correlation effects. The atomic configurations of the lowest-energy isomers obtained at the DFT level, were further used to calculate the total energy at the MP2/6-31G(d) level of theory. The comparison of the energetics between these two methods suggests that while the LDA formalism overestimates the binding energies, MP2 results provide underestimated values as compared to the experimental observations. The geometries of the Al substituted Si clusters are almost similar as that of the homoatomic Si cluster except replacing one Si atom with an Al atom at different sites. A brief comparison for different ground-state geometries between $Si_n$ and $Si_{n-1}Al$ clusters reveals that the lowest-energy structure of the $Si_5$ cluster is an elongated TBP but $Si_4Al$ cluster favors capped bent rhombus. For $Si_6$, both crossed rhombus ($D_{4h}$) and edge capped TBP ($C_{2v}$) are isoenergetic. The corresponding Al substituted $Si_5Al$ cluster shows an edge capped TBP is energetically more favorable than the crossed rhombus. The ground-state structure of $Si_8$ and the $Si_7Al$ also differs in a way where the $Si_8$ corresponds to a distorted bicapped octahedron but the $Si_7Al$ cluster shows the capped PBP is the most favored structure. The trend in the binding energy is similar for both $Si_n$ and $Si_{n-1}Al$ clusters with $n=4$, 6, and 10 as the most stable clusters in these series. This reflects the magic behavior of these clusters. The vertical ionization potentials of $Si_n$ and $Si_{n-1}Al$ clusters were calculated from the difference in the total energies between neutral and positively charged ions having same atomic configurations. The inclusion of Al atom in the $Si_n$ cluster matrix reduces the ionization potentials by lifting up the HOMO energy levels at lower values. The analysis of the fragmentation energy for $Si_n$ and $Si_{n-1}Al$ cluster shows that the energy required to dissociate a Si atom is higher than that of Al. However, the energy required to dissociate a Si atom from $Si_{n-1}Al$ is higher than $Si_n$ for $n=4$, 6, 8, 10, and 11. Thus we infer that although the incorporation of an Al atom in Si cluster matrix reduces its average binding energy it improves the bond strength between Si atoms.

*Email: chimaju@magnum.barc.ernet.in

[1] M. F. Jarrold, Science **252**, 1085 (1991).
[2] W. L. Brown, R. R. Freeman, K. Raghavachari, and M. Schluter, Science **235**, 860 (1987).
[3] S. Hayashi, Y. Kanzawa, M. Kataoka, T. Nagarede, and K. Yamamoto, Z. Phys. D: At., Mol. Clusters **26**, 144 (1993).
[4] L. A. Bloomfield, R. R. Freeman, and W. L. Brown, Phys. Rev. Lett. **54**, 2246 (1985).
[5] L. A. Bloomfield, M. E. Guesic, R. R. Freeman, and W. L. Brown, Chem. Phys. Lett. **121**, 33 (1985).
[6] K. D. Rinnen and M. L. Mandich, Phys. Rev. Lett. **69**, 1823 (1992).
[7] W. Begemann, K. H. Meiwes-Broer, and H. O. Lutz, Phys. Rev. Lett. **73**, 2248 (1986).
[8] M. F. Jarrold and E. C. Honea, J. Phys. Chem. **95**, 9181 (1991).
[9] J. M. Hunter, J. L. Fye, M. F. Jarrold, and J. E. Bower, Phys. Rev. Lett. **73**, 2063 (1994).
[10] T. P. Martin and H. Schaber, J. Chem. Phys. **83**, 855 (1985).
[11] O. Cheshnovsky, S. H. Yang, C. L. Pettiette, M. J. Craycraft, Y. Liu, and R. E. Smalley, Chem. Phys. Lett. **138**, 119 (1987).
[12] E. C. Honea, A. Ogura, D. R. Peale, C. Felix, C. A. Murray, K. Raghavachari, W. O. Sprenger, M. F. Jarrold, and W. L. Brown, J. Chem. Phys. **110**, 12161 (1999).
[13] M. F. Jarrold and W. L. Brown, Nature (London) **366**, 42 (1993).
[14] S. Li, R. J. Van Zee, W. Weltner, and K. Raghavachari, Jr., Chem. Phys. Lett. **243**, 275 (1995).
[15] K. Raghavachari and V. Logovinsky, Phys. Rev. Lett. **55**, 2853 (1985).
[16] K. Raghavachari, J. Chem. Phys. **84**, 5672 (1986).
[17] K. Raghavachari and C. M. Rohlfing, J. Chem. Phys. **89**, 2219 (1988).
[18] C. M. Rohlfing and K. Raghavachari, Chem. Phys. Lett. **167**, 559 (1990); J. Chem. Phys. **96**, 2114 (1992).
[19] K. Raghavachari and C. M. Rohlfing, Chem. Phys. Lett. **94**, 3670 (1991).
[20] K. Raghavachari and C. M. Rohlfing, Chem. Phys. Lett. **198**, 521 (1992).
[21] K. M. Ho, A. A. Shvartsburg, B. Pan, Z. Y. Lu, C. Z. Wang, J. G. Wacker, J. L. Fye, and M. F. Jarrold, Nature (London) **392**, 582 (1998); M. F. Jarrold and V. A. Constant, Phys. Rev. Lett. **67**, 2994 (1991); M. F. Jarrold and J. E. Bower, J. Phys. Chem. **96**, 9180 (1992).

[22] H. Haberland, *Clusters of Atoms and Molecules: Theory, Experiment, and Clusters of Atoms* (Springer-Verlag, New York, 1994).
[23] B. Liu, Z. Y. Lu, B. Pan, C.-Z. Wang, K.-M. Ho, A. A. Shvartsburg, and M. F. Jarrold, J. Chem. Phys. **109**, 9401 (1998); Z. Y. Lu, C. Z. Wang, and K. M. Ho, Phys. Rev. B **61**, 2329 (2000).
[24] B. X. Li, P. L. Cao, and M. Jiang, Phys. Status Solidi B **218**, 399 (2000); B. X. Li and P. L. Cao, Phys. Rev. A **62**, 023201 (2000); J. Phys.: Condens. Matter **13**, 1 (2001).
[25] S. Wei, B. N. Barnett, and U. Landman, Phys. Rev. B **55**, 7935 (1997).
[26] I. Vasiliev, S. Ogut, and J. R. Chelikowsky, Phys. Rev. Lett. **78**, 4805 (1997).
[27] A. Hiraki, Surf. Sci. **168**, 74 (1986).
[28] A. A. Istratov and E. R. Weber, Appl. Phys. A: Mater. Sci. Process. **66**, 123 (1998).
[29] U. Wahl, A. Vantomme, G. Langouche, J. G. Correia, and ISOLDE Collaboration, Phys. Rev. Lett. **84**, 1495 (2000).
[30] A. Zunger and U. Lindefeldt, Phys. Rev. B **26**, 5989 (1982).
[31] F. Beeler, O. K. Andersen, and M. Scheffler, Phys. Rev. B **41**, 1603 (1990).
[32] D. E. Woon, D. S. Marynick, and S. K. Estreicher, Phys. Rev. B **45**, 13 383 (1992).
[33] S. K. Estreicher, Phys. Rev. B **60**, 5375 (1999).
[34] S. M. Beck, J. Chem. Phys. **90**, 6306 (1989).
[35] J. J. Scherer, J. B. Paul, C. P. Collier, and R. J. Saykally, J. Chem. Phys. **102**, 5190 (1995).
[36] J. J. Scherer, J. B. Paul, C. P. Collier, and R. J. Saykally, J. Chem. Phys. **103**, 113 (1995).
[37] J. J. Scherer, J. B. Paul, C. P. Collier, A. O'Keefe, and R. J. Saykally, J. Chem. Phys. **103**, 9187 (1995).
[38] H. Hiura, T. Miyazaki, and T. Kanayama, Phys. Rev. Lett. **86**, 1733 (2001); Phys. News Update **527**, Feb (2001).
[39] J. G. Han and Y. Y. Shi, Chem. Phys. **266**, 33 (2001).
[40] J. G. Han and F. Hagelberg, J. Mol. Struct.: THEOCHEM **549**, 165 (2001).
[41] J. G. Han and F. Hagelberg, Chem. Phys. **263**, 255 (2001).
[42] J. G. Han, C. Xiao, and F. Hagelberg, Struct. Chem. **13**, 173 (2002).
[43] C. Xiao and F. Hagelberg, J. Mol. Struct.: THEOCHEM **529**, 241 (2000); C. Xiao, F. Hagelberg, I. Ovcharenko, and W. A. Lester, Jr., *ibid.* **549**, 181 (2001).
[44] C. Xiao, F. Hagelberg, and W. A. Lester, Jr., Phys. Rev. B **66**, 075425 (2002).
[45] I. V. Ovcharenko, W. A. Lester, Jr., C. Xiao, and F. Hagelberg, J. Chem. Phys. **114**, 9028 (2001).
[46] K. Jackson and B. Nellermoe, Chem. Phys. Lett. **254**, 249 (1996).
[47] T. Nagano, K. Tsumuraya, H. Eguchi, and D. J. Singh, Phys. Rev. B **64**, 155403 (2001).
[48] V. Kumar and Y. Kawazoe, Phys. Rev. Lett. **87**, 045503 (2001).
[49] V. Kumar and Y. Kawazoe, Phys. Rev. B **65**, 073404 (2002).
[50] J. Liu and S. Nagase, Phys. Rev. Lett. **90**, 115506 (2003); V. Kumar and Y. Kawazoe, *ibid.* **90**, 055502 (2003); Q. Sun, Q. Wang, P. Jena, B. K. Rao, and Y. Kawazoe, *ibid.* **90**, 135503 (2003).
[51] R. Kishi, S. Iwata, A. Nakajima, and K. Kaya, J. Chem. Phys. **107**, 3056 (1997).
[52] U. Landman, R. N. Barnett, A. G. Scherbakov, and P. Avouris, Phys. Rev. Lett. **85**, 1958 (2000).
[53] V. G. Kotlyar, A. V. Zotov, A. A. Saranin, T. V. Kasyanova, M. A. Cherevik, I. V. Pisarenko, and V. G. Lifshits, Phys. Rev. B **66**, 165401 (2002).
[54] M. Paulose, C. A. Grimes, O. K. Varghese, and E. C. Dickey, Appl. Phys. Lett. **81**, 153 (2002).
[55] J. Hutter *et al.*, CPMD Version 3.5.3., IBM Zurich Research Laboratory and MPI für Festkörperforschung.
[56] G. B. Bachelet, D. R. Hamann, and M. Schluter, Phys. Rev. B **26**, 4199 (1982).
[57] L. Kleinman and D. M. Bylander, Phys. Rev. Lett. **48**, 1425 (1982).
[58] D. M. Ceperley and B. J. Alder, Phys. Rev. Lett. **45**, 566 (1980).
[59] M. Haser, J. AlmLof, and G. E. Scuseria, Chem. Phys. Lett. **181**, 497 (1991).
[60] C. Møller and M. S. Plesset, Phys. Rev. **46**, 618 (1934).
[61] W. J. Hehre, L. Radom, P. Von R. Schleyer, and J. A. Pople, *Ab Initio Molecular Orbital Theory* (Wiley, New York, 1985).
[62] M. W. Schmidt, K. K. Baldridge, J. A. Boatz, S. T. Elbert, M. S. Gordon, J. H. Jensen, S. Koseki, N. Matsunaga, K. A. Nguyen, S. J. Su, T. L. Windus, M. Dupuis, and J. A. Montgomery, J. Comput. Chem. **14**, 1347 (1993).
[63] J. C. Grossman and L. Mitas, Phys. Rev. Lett. **74**, 1323 (1995); L. Mitas, J. C. Grossman, I. Stich, and J. Tobik, *ibid.* **84**, 1479 (2000).
[64] X. Zhu and X. C. Zenga, J. Chem. Phys. **118**, 3558 (2003).
[65] C. Xiao, F. Hagelberg, and W. A. Lester, Jr., Phys. Rev. B **66**, 075425 (2002).
[66] P. W. Atkins, *Molecular Quantum Mechanics*, 3rd ed. (Oxford University Press, Oxford, 1997); Ref. 2; R. T. Morrison and R. N. Boyd, *Organic Chemistry*, 6th ed. (Prentice-Hall, New York, 1992).
[67] L. A. Bloomfield, R. R. Freeman, and W. L. Brown, Phys. Rev. Lett. **54**, 2246 (1985).
[68] C. Majumder, V. Kumar, H. Mizuseki, and Y. Kawazoe, Phys. Rev. B **64**, 233405 (2001).
[69] *CRC Handbook of Chemistry and Physics*, 49th ed., edited by R. C. Weast (CRC Press, Cleveland, Ohio, 1969).
[70] K. Fuke, K. Tsukamoto, F. Misaizu, and M. Sanekata, J. Chem. Phys. **99**, 7807 (1993).